BJP British Journal of Pharmacology

DOI:10.1111/j.1476-5381.2011.01384.x
www.brjpharmacol.org

RESEARCH PAPER

The cannabinoid receptor inverse agonist AM251 regulates the expression of the EGF receptor and its ligands via destabilization of oestrogen-related receptor α protein

JL Fiori[1], M Sanghvi[1], MP O'Connell[2], SM Krzysik-Walker[1], R Moaddel[1] and M Bernier[1]

[1]*Laboratory of Clinical Investigation and* [2]*Laboratory of Molecular Biology and Immunology, National Institute on Aging, National Institutes of Health, Baltimore, MD, USA*

Correspondence
Dr Michel Bernier, National Institute on Aging, National Institutes of Health, 251 Bayview Boulevard, Suite 100, Baltimore, MD 21224-6825, USA. E-mail: bernierm@mail.nih.gov

Keywords
cancer; cell cycle; cell invasion; colony formation; EGF receptor; inverse agonist; orphan nuclear hormone receptors; signal transduction

Received
19 August 2010
Revised
24 February 2011
Accepted
20 March 2011

BACKGROUND AND PURPOSE

AM251 is an inverse agonist of the cannabinoid 1 receptor (CB_1R) that can exert 'off-target' effects *in vitro* and in CB_1R knock-out mice. AM251 is also potent at modulating tumour cell growth, suggesting that growth factor-mediated oncogenic signalling could be regulated by AM251. Since dysregulation of the EGF receptor has been associated with carcinogenesis, we examined AM251 regulation of EGF receptor (EGFR) expression and function.

EXPERIMENTAL APPROACH

The various biological functions of AM251 were measured in CB_1R-negative human cancer cells. Pharmacological and genetic approaches were used to validate the data.

KEY RESULTS

The mRNA levels for EGFR and its associated ligands, including HB-EGF, were induced several fold in PANC-1 and HCT116 cells in response to AM251. This event was associated with enhanced expression of EGFR on the cell surface with concomitant increase in EGF-induced cellular responses in AM251-treated cells. Exposure to XCT790, a synthetic inverse agonist of the orphan nuclear oestrogen-related receptor α (ERRα), also induced EGFR and HB-EGF expression to the same extent as AM251, whereas pretreatment with the ERRα-selective agonist, biochanin A, blunted AM251 actions. AM251 promoted the degradation of ERRα protein without loss of the corresponding mRNA. Knock-down of ERRα by siRNA-based approach led to constitutive induction of EGFR and HB-EGF levels, and eliminated the biological responses of AM251 and XCT790. Finally, AM251 displaced diethylstilbestrol prebound to the ligand-binding domain of ERRα.

CONCLUSIONS AND IMPLICATIONS

AM251 up-regulates EGFR expression and signalling via a novel non-CB_1R-mediated pathway involving destabilization of ERRα protein in selected cancer cell lines.

Abbreviations

4-OHT, 4-hydroxytamoxifen; AM251, 1-(2,4-dichlorophenyl)-5-(4-iodophenyl)-4-methyl-N-1-piperidinyl-1H-pyrazole-3-carboxamide; AM630, [6-iodo-2-methyl-1-[2-(4-morpholinyl)ethyl]-1H-indol-3-yl](4-methoxyphenyl)-methanone; CB_1R, cannabinoid 1 receptor; DES, diethylstilbestrol; DY131, N-[(E)-[4-(diethylamino)phenyl]methylideneamino]-4-hydroxybenzamide; EGFR, EGF receptor; ERR, oestrogen-related receptor; IR α-sub, insulin receptor α-subunit; LBD,

ligand-binding domain; NRIP1, receptor-interacting protein 140; PGC-1α, peroxisome proliferator-activated receptor co-activator-1 alpha; PIAS4, protein inhibitor of activated signal transducer and activator of transcription-γ; SERMs, selective oestrogen receptor modulators; siRNA, silencing RNA; WIN 55212-2, [(3R)-2,3-dihydro-5-methyl-3-(4-morpholinylmethyl)pyrrolo[1,2,3-de]-1,4-benzoxazin-6-yl]-1-naphthalenyl-methanone; XCT790, (2*E*)-3-(4-{[2,4-bis (trifluoromethyl)benzyl]oxy}-3-methoxyphenyl)-2-cyano-*N*-[5-(trifluoromethyl)-1,3,4-thiadiazol-2-yl]acrylamide

Introduction

The EGF receptor (EGFR) and its naturally occurring ligands play a key role in oncogenesis and migration (Maa *et al.*, 1995; Greulich *et al.*, 2005). The data in the oncomine cancer profiling database (http://www.oncomine.org) indicate that a large portion of human cancers express EGFR and its ligands to a greater extent than in non-malignant tissues. Several tumour cell types require an EGFR-mediated autocrine pathway for proliferation (Murphy *et al.*, 2001; Nicholson *et al.*, 2001), and ectodomain shedding of transmembrane EGF ligands by metalloproteases accounts for increased migration, invasion and angiogenesis upon stimulation of GPCRs (Bhola and Grandis, 2008; Paolillo and Schinelli, 2008). The anti-proliferative action of the endocannabinoid anandamide depends on growth factor receptor down-regulation in human breast and prostate cancer cell lines (Melck *et al.*, 2000; Mimeault *et al.*, 2003). In contrast, a recent report indicates the growth-promoting effect of cannabinoids via the transactivation of the EGFR in several tumour cell lines (Hart *et al.*, 2004). Interestingly, changes in expression of specific G protein-coupled cannabinoid receptors, CB_1R and CB_2R have been shown to occur during carcinogenesis. It is suggested that the CB_1R levels may be suppressed in breast tumours (Caffarel *et al.*, 2006), whereas in prostate cancer cells, there is an up-regulation of both CB_1R and CB_2R compared to non-malignant cells (Sarfaraz *et al.*, 2005). Although the CB_1R is ubiquitously expressed, the CB_2R expression is largely limited to the immune system. A number of CBR-dependent and -independent mechanisms have been proposed for the anti-proliferative effects of endocannabinoids and phytocannabinoids (Ruiz *et al.*, 1999; Ramer *et al.*, 2001; Patsos *et al.*, 2005); however, it is unclear whether the expression of EGFR and/or activation of the EGFR signalling pathway is altered in response to changes in constitutive and ligand-induced CB_1R activity, and whether this can affect tumourigenesis and cell growth potential of selected cancer cell lines.

Earlier studies have established a link between selective oestrogen receptor modulators (SERMs), which include 4-hydroxytamoxifen (4-OHT), and EGFR transcription in HeLa cells (Salvatori *et al.*, 2003) and U2OS osteosarcoma cells (Salvatori *et al.*, 2009). In the latter study, the authors reported that treatment with 4-OHT regulates the EGFR level in an oestrogen receptor isoform-specific manner. However, 4-OHT has also been reported to be an inverse agonist for the orphan nuclear receptor, oestrogen-related receptor γ (ERRγ) (Coward *et al.*, 2001; Tremblay *et al.*, 2001a). Moreover, the synthetic oestrogen diethylstilbestrol (DES) binds to and inhibits ERRα and ERRγ activities (Tremblay *et al.*, 2001b), and neonatal exposure to DES alters the normal EGFR expression levels in adult mouse reproductive tract (Iguchi *et al.*, 1993). Hence, it is suggested that SERMs can directly control proliferation and modulate EGFR expression via the orphan nuclear ERRs.

The initial purpose of this study was to delineate the role of the synthetic CB_1R inverse agonist, AM251, in the regulation of EGFR and its ligands in a panel of four human cancer cells in culture that express very low levels of CB_1R. Earlier studies have described CB_1R-independent actions of AM251 and its structurally related clinical analogue, rimonabant, in wild-type (Di *et al.*, 2005; Rodgers *et al.*, 2005) and CB_1R knock-out mice (Bukoski *et al.*, 2002; Bátkai *et al.*, 2004; Jin *et al.*, 2004). Here, we observed a potent and co-ordinate induction in the expression of EGFR and its ligands by AM251 in the human PANC-1 pancreatic cancer cell line and HCT116 colon carcinoma cells, but not in DLD1 and MDA-MD-468 carcinoma cells. Additional experiments were performed to provide new mechanistic insights into the actions of AM251. The results derived from our pharmacological and molecular biological studies indicated a novel interaction between AM251 and ERRα, which was associated with inhibition of ERRα target gene expression and proteolytic degradation of this orphan nuclear receptor. Further investigations revealed that AM251 displaces DES prebound to the recombinant ERRα ligand-binding domain (LBD) immobilized on a chromatographic support. The functional consequences of ERRα inhibition by AM251 and related compounds might be significant in EGFR-mediated proliferation of cancer cells.

Methods

Maintenance and treatment of cell lines

Human PANC-1 cells (ATCC, Manassas, VA, USA) were maintained in Dulbecco's modified Eagle's medium (DMEM) medium (Gibco, Carlsbad, CA, USA) supplemented with 4.5 $g \cdot L^{-1}$ D-glucose, 4 mM L-glutamine, 1 mM sodium pyruvate, 1.5 $g \cdot L^{-1}$ sodium bicarbonate, penicillin/streptomycin and 10% fetal bovine serum (FBS; HyClone, Logan, UT, USA). Human HCT116 and DLD1 cells were maintained in McCoy's 5a medium (Gibco) supplemented with 4 mM L-glutamine, penicillin–streptomycin and 10% FBS. Human MDA-MB-468 cells were maintained in DMEM/F12 medium (Gibco) supplemented with 4 mM L-glutamine, penicillin/streptomycin and 10% FBS. HCT-116, DLD-1 and MDA-MB-468 cells were obtained from Dr Patrice Morin at the National Institute on Aging (NIA, Baltimore, MD, USA). All cell lines were cultured at 37°C in 5% CO_2, and the medium was replaced every 2–3 days.

Unless otherwise indicated, cells were deprived of serum for 3 h, followed by the addition of 5 μM AM251, AM630 or WIN 55212-2 (Cayman Chemical, Ann Arbor, MI, USA) for 24 h. To examine the ERRα and ERRγ agonists and inverse

agonists, cells were deprived of serum for 3 h, followed by the addition of 100 nM biochanin A (INDOFINE Chemical Company, Hillsborough, NJ, USA), 1.5 μM XCT790 (Sigma-Aldrich, St. Louis, MO, USA), 100 nM DY131 (Tocris Bioscience, Ellisville, MO, USA) or 1 μM 4-OHT (Sigma-Aldrich) for 24 h. Dose–response curves were performed with 0–5 μM AM251, 0–1 μM biochanin A, 0–5 μM XCT790 and 0–20 μM DES (Sigma-Aldrich) for 24 h. To examine whether biochanin A can block the effects of AM251, cells were deprived of serum for 3 h, pretreated with 1 μM biochanin A for 1 h, followed by treatment with 5 μM of AM251 for 24 h.

ERRα gene silencing by siRNA

PANC-1 cells were reverse transfected in 35 mm dishes with 50 nM of negative control or ERRα siRNA (Qiagen, Valencia, CA, USA) for 24 h using 7.5 μL of Lipofectamine RNAiMAX reagent (Invitrogen, Carlsbad, CA, USA) following the manufacturer's protocol. Qiagen's HP GenomeWide siRNAs were designed using HP OnGuard siRNA Design, and have been validated to perform efficient knock-down with minimal off-target effects. The sequences for ERRα siRNA were: 5′-GAGAGAUUGUGGUCACCAUTT-3′ (sense strand) and 5′-AUGGUGACCACAAUCUCUCGG-3′ (antisense strand). The sequences for negative control siRNA are proprietary. Following 24 h of siRNA knock-down, cells were washed with PBS; deprived of serum for 3 h; and treated with dimethyl sulphoxide (DMSO), AM251 or XCT790 for 24 h.

RNA extraction, cDNA synthesis and quantitative PCR

RNA was extracted using TRIzol (Invitrogen) and an RNeasy Mini kit (Qiagen) according to the manufacturer's instructions. Using 1 μg RNA, cDNA was synthesized using qScript cDNA SuperMix (Quanta Biosciences, Gaithersburg, MD, USA). Gene expression was quantified using the SYBR green (Quanta Biosciences) method of real-time PCR, and mRNA levels were compared to standard curves and normalized to 18S mRNA. PCR reactions were performed in triplicate with Universal 18S primers (Ambion, Austin, TX, USA) or 100 nM of each gene-specific primer. The primers for human EGFR [forward (5′-AGGACCAAGCAACATGGTCA-3′) and reverse (5′-CCTTGCAGCTGTTTTGACCT-3′)], HB-EGF [forward (5′-CCCTCCCACTGTATCCACG-3′) and reverse (5′-AGTGAC TCTCAAAAGGTCCAGA-3′)], CB1R #1 [forward (5′-CTGTG CGTCATCCTCCACTC-3′) and reverse (5′-AAACACGTTGC GGCTATCTTT-3′)], CB1R #2 [forward (5′-AAGGTGACATGGC ATCCAAAT-3′) and reverse (5′-AGGACGAGAGAGACTTGTT GTAA-3′)], and PDK4 [forward (5′-AGTTGACCCAGTCACCA ATCA-3′) and reverse (5′-TCACAGTTAGGATCAATGCTTCC-3′)] (Integrated DNA Technologies, Coralville, IA, USA) were designed to cross intron–exon junctions. The primers for human ERRα and ERRγ were purchased from SABiosciences (Frederick, MD, USA). For comparative analysis, human brain total RNA was purchased from Ambion. Quantitative PCR was performed on an ABI Prism 7300 (Applied Biosystems, Foster City, CA, USA) sequence detection system using standard conditions.

RT² profiler PCR array system

PANC-1 cells were deprived of serum for 3 h, followed by the addition of DMSO or 5 μM of AM251 for 24 h. RNA was extracted as described above, and using 1 μg RNA, cDNA was synthesized using an RT² First Strand Kit (SABiosciences). Following the manufacturer's protocol, real-time PCR reactions were run in a 96-well Human EGF/PDGF Signaling plate (SABiosciences) using SABiosciences RT² qPCR Master Mix. All recommended quality controls were performed, and the $\Delta\Delta C_t$ method of data analysis was carried out on SABiosciences PCR Data Analysis Web Portal (http://www.SABiosciences.com/pcrarraydataanalysis.php).

Western blotting and densitometry

Cells were lysed in RIPA buffer (25 mM HEPES, 134 mM NaCl, 1% NP-40, 0.1% SDS, 1 mM sodium othovanadate, 0.5% sodium deoxycholate, 100 mM NaF) supplemented with protease inhibitor cocktail set I and phosphatase inhibitor cocktail set II (Calbiochem, Gibbstown, NJ, USA) for 20 min on ice with occasional vortexing, and then pelleted in a microcentrifuge at maximum speed for 20 min to remove insoluble material. Cell lysates were resolved on 4–12% Tris–glycine gels (Invitrogen) and blotted onto polyvinylidene difluoride membranes using the iBlot (Invitrogen). The blots were blocked in TBST [10 mM Tris–HCl (pH 8.0), 150 mM NaCl, 0.1% Tween 20] supplemented with either 5% non-fat milk or 5% BSA for 1 h at room temperature, and the primary antibodies were added at 1:1000 in blocking buffer for 16 h at 4°C. The antibodies were raised against EGFR, D-glyceraldehyde-3-phosphate dehydrogenase (GAPDH) and insulin receptor α-subunit (IR α-sub) (Santa Cruz Biotechnology, Santa Cruz, CA, USA); β-tubulin, Akt and phosphoactive Akt (Cell Signaling Technology, Danvers, MA, USA); ERRα (Abcam, Cambridge, MA, USA); and phosphotyrosine clone 4G10 (1:2000, Millipore, Billerica, MA, USA). Membranes were washed with TBST, and the appropriate secondary antibody (1:5000, GE Heathcare, Piscataway, NJ, USA) was added in 5% non-fat milk/TBST for 1 h at room temperature with agitation. Membranes were washed again with TBST and developed using ECL (GE Heathcare). Western blot images were scanned, saved as tiff files, inverted and integrated density was analysed using ImageJ software (National Institutes of Health, Bethesda, MD, USA). Values were normalized to either β-tubulin or GAPDH.

Cell surface protein isolation

Biotinylation and isolation of cell surface proteins were performed using a cell surface protein isolation kit (Thermo Scientific, Rockford, IL, USA) following the manufacturer's protocol. Briefly, PANC-1 cells were grown in four T75 flasks to 90–95% confluence, deprived of serum for 3 h, treated with DMSO or 5 μM of AM251 for 24 h and labelled with EZ-link sulpho-NHS-SS-biotin. The cells were subsequently lysed, sonicated on low power and incubated for 30 min on ice. The labelled proteins were then isolated using NeutrAvidin Agarose, and the bound proteins were released by incubating with SDS–PAGE sample buffer containing 50 mM DTT. Samples were analysed by Western blot.

Flow cytometry to analyse cell surface EGFR levels

PANC-1 cells were deprived of serum for 3 h followed by treatment with DMSO or 5 μM AM251 for 24 h, after which

the medium was removed and cells were rinsed three times with ice-cold PBS, 0.5 M EDTA. Cells were detached from the plates by scraping, collected into conical tubes and sedimented at 1300 rpm before resuspension in incubation buffer (PBS, 2% IgG-free BSA) at a concentation of 1×10^7 cells·mL^{-1}. Aliquots (100 µL) were transferred to new tubes and incubated with 0.5 µg of anti-EGFR (Santa Cruz Biotechnology) or 1 µg control mouse PE-labelled IgG_{2a} (Santa Cruz Biotechnology) for 30 min at 4°C in the dark. Cells were washed three times followed by the addition of PE-labelled donkey anti-mouse IgG (1:250, Jackson ImmunoResearch Laboratories, West Grove, PA, USA) in incubation buffer for 30 min at 4°C in the dark. Stained cells were washed in incubation buffer and fixed with 1 mL of 1% paraformaldehyde in PBS. After being mixed several times, the cell suspension was passed through a 70 µm nylon mesh filter (BD Biosciences, San Jose, CA, USA) and analysed with the use of a BD FACSCalibur flow cytometer (BD Biosciences).

Propidium iodide staining for DNA cell cycle analysis

PANC-1 cells were deprived of serum for 3 h, treated with DMSO or 5 µM AM251 for 24 h and then incubated with 20 nM of recombinant human EGF (Millipore) for 6 h. In a second series of experiments, PANC-1 and HCT116 cells were transfected with control non-targeting siRNA or ERRα siRNA for 24 h as described above, deprived of serum for 3 h and then treated with DMSO, 5 µM AM251 or 1.5 µM XCT790 for 24 h The medium was collected and transferred into a 15 mL conical tube on ice. Cells were washed with PBS, trypsinized and collected into the conical tubes containing the medium. After centrifugation, the cell pellets were gently resuspended in PBS to break up clumps, and cell cycle analysis was performed on propidium iodide-stained nuclei prepared using the NIM procedure (Wersto and Stetler-Stevenson, 1995). The BD FACSCalibur flow cytometer was used for cell cycle analysis.

Matrigel invasion assays

Invasion assays were performed using transwell migration chambers (Corning Life Sciences, Lowell, MA, USA). Filters (8 µM) were coated with 150 µL of 80 µg·mL^{-1} of reconstituted basement membrane (Matrigel) (BD Biosciences). Then, 1×10^5 cells were seeded onto the filters, the cells were deprived of serum for 3 h and then treated with DMSO or 5 µM AM251 for 24 h. EGF (20 nM) was then added to the appropriate wells, and 20% FBS was placed in the lower chamber to act as a chemo-attractant. Cells were allowed to invade and adhere to the lower chamber for 72 h, after which they were stained using crystal violet; images were taken, and cells were counted.

Soft agar colony formation

Colony formation in soft agar was measured using the CytoSelect 96-well cell transformation assay (Cell Biolabs, San Diego, CA, USA) following the manufacturer's protocol. Briefly, a base agar layer (50 µL) containing an equal volume of 1.2% agar solution and 2× DMEM/20% FBS medium was added to a flat bottom microplate, followed by a cell agar layer (75 µL) containing an equal volume of 1.2% agar solution, 2× DMEM/20% FBS medium and DMSO- or AM251-treated PANC-1 cell suspension ($0.5–4 \times 10^5$ cells·mL^{-1}). An aliquot of culture medium (100 µL) was added to each well, and 20 nM of EGF was added to the appropriate wells. The cells were incubated for 7 days at 37°C and 5% CO_2, after which the agar was solubilized, and cells were lysed and detected with CyQuant GR dye using a 485/520 nm filter set on a GloMax-Multi Detection System (Promega, Madison, WI, USA).

Chromatographic studies with immobilized ERRα LBD

The LBD of ERRα was immobilized using a previously described procedure (Marszałł *et al.*, 2008; Sanghvi *et al.*, 2010) and packed into a Tricorn 5/20 glass column (50 × 5 mm I.D., GE Healthcare Bio-Sciences AB, Piscataway, NJ, USA). The column was washed with Tris–HCl buffer (10 mM, pH 7.4) for 2 h at 0.2 mL·min^{-1} at 25°C.

The frontal chromatographic studies were performed as recently described (Sanghvi *et al.*, 2010) on a series 1100 liquid chromatography/mass selective detector (Agilent Technologies, Palo Alto, CA, USA). The chromatographic system was interfaced to a 250 MHz Kayak XA computer (Hewlett-Packard, Palo Alto, CA, USA) using ChemStation software (Rev B.10.00, Hewlett-Packard). The mobile phase was composed of ammonium acetate (10 mM, pH 7.4) containing 10% methanol, and the experiments were carried out at a flow rate of 0.5 mL·min^{-1}. DES was monitored using single-ion monitoring (M-1) at *m/z* values 267.2. Serial concentrations of AM251 (0.05, 0.1, 0.25, 0.5, 0.75, 1.0 and 2.0 µM) and biochanin A (0.1, 0.25, 0.5 and 0.75 µM) were prepared in the mobile phase. The observed retention volumes were used to calculate binding affinity of AM251 ($I_{ERR\alpha}$) using a previously described approach, Eqn 1 (Moaddel and Wainer, 2009):

$$[I_{ERR\alpha}](V - V_{min}) = B_{max}[I_{ERR\alpha}].\{(K_{IERR\alpha}[I_{ERR\alpha}]\}^{-1} \quad (1)$$

where V is the retention volume of $I_{ERR\alpha}$ measured at the midpoint of the breakthrough curve, V_{min} is the retention volume of $I_{ERR\alpha}$ in the highest concentration applied of the displacer ligand and B_{max} is number of active binding sites of the immobilized target. The binding affinity values were obtained by plotting $[I_{ERR\alpha}](V - V_{min})$ versus $[I_{ERR\alpha}]$, and the data were analysed by non-linear regression with the sigmoidal response curve using Prism 4 software (Graph Pad Software Inc., San Diego, CA, USA).

Statistical analysis

Results are presented as means ± SD unless otherwise specified. Statistical analysis was performed by Student's *t*-test, and values of $P < 0.05$ were considered significant.

Results

CB_1R-independent up-regulation of EGFR and its ligands by AM251

To assess the relative expression of CB_1R in a panel of high EGFR-expressing cancer cell lines, quantitative PCR was per-

formed using primers that recognize both isoform a (primer set 1) and isoform b (primer set 2) of CB_1R (Figure 1A). All cancer cell lines, which included human pancreatic adenocarcinoma (PANC-1), human colorectal carcinomas (DLD1 and HCT116) and human breast adenocarcinoma (MDA-MB-468), had very weak CB_1R mRNA expression when compared to human brain mRNA, which was used as a positive control (Herkenham *et al.*, 1991; Matsuda *et al.*, 1993). Three additional sets of primers were also tested and no significant amounts of CB_1R mRNA were detected (data not shown). This result was confirmed by Western blot analysis, which did not detect CB_1R protein in any of the cancer cell lines used in the study (data not shown).

The compound AM251, described as a CB_1R inverse agonist, is also able to elicit CB_1R-independent responses. In order to determine the potential role of AM251 on EGFR-mediated oncogenic signalling, an EGF/PDGF signalling pathway PCR array (SABiosciences, #PAHS-040) was used. Exposure of PANC-1 cells to AM251 (5 μM) for 24 h resulted in an up-regulation of EGFR and HB-EGF mRNA levels by 6.7- and 14.0-fold, respectively, when compared to control (Supporting Information Table S1). Quantitative PCR analysis indicated that PANC-1 and HCT116 cells responded to AM251 treatment with a 7.7 ± 1.0- and 8.6 ± 1.2-fold increase in HB-EGF mRNA levels versus control, respectively. In contrast, the responsiveness of DLD1 and MDA-MB-468 cells to AM251 was much lower with only a 1.1 ± 0.1- and 2.3 ± 0.3-fold increase over control, respectively (Figure 1B). From these results, we performed the following series of experiments only in PANC-1 and HCT116 cells, the latter used mostly to validate the PANC-1 data.

When PANC-1 cells were treated with AM251, the expression of EGFR and HB-EGF mRNA was effectively increased in a time-dependent fashion, with the half-maximum effect observed after a 7 h treatment with AM251 (Figure 1C). The mRNA levels for other EGFR ligands, such as betacellulin and epiregulin, were also up-regulated in AM251-treated PANC-1 cells versus control, whereas the insulin-like growth factor 1 receptor mRNA was unaffected (data not shown). In the presence of the synthetic cannabinoid receptor agonist WIN 55212-2, EGFR and HB-EGF mRNA expression was similar to control (Supporting Information Figure S1A). Western blot analysis showed that exposure of PANC-1 cells to AM251 resulted in 2.8 ± 0.3-fold increase in EGFR protein levels over control (Figure 1D), and the results were similar in HCT116 cells (Figure 1E). In contrast, neither WIN 55212-2 nor the specific CB_2R antagonist AM630 altered the expression of EGFR when compared to vehicle-treated PANC-1 cells (Supporting Information Figure S1B and C).

To evaluate the cellular distribution of EGFR, cell surface proteins were biotinylated, captured on an agarose column, eluted and analysed by Western blot analysis. Treatment of PANC-1 cells with AM251 resulted in an 2.2-fold increase in EGFR expression at the cell surface versus control, and under these conditions the IR α-sub levels remained unchanged (Figure 1F). The lack of GAPDH signal indicated that the membrane extracts were free of cytosolic proteins. These results were confirmed independently by flow cytometry of intact cells using anti-EGFR antibody coupled with PE-labelled secondary antibody (Supporting Information Figure S2). The FACS analysis showed a significant rightward shift in the peak of the AM251-treated samples versus control, with the mean fluorescent staining increasing from 528 ± 24 to 724 ± 28 ($P < 0.01$, $n = 4$).

Effect of AM251 on EGF-induced EGFR activation and stimulation of biological responses in PANC-1 cells

Serum-starved PANC-1 cells were incubated with various concentrations of EGF for 5 min, and the total lysates were analysed by Western blotting. AM251-treated cells exhibited a dose-dependent increase in ligand-mediated EGFR tyrosine phosphorylation that was ~2.5-fold higher than that observed in control (Figure 2A, upper panel). However, densitometry analysis showed that the ratio of phosphorylated to total EGFR was not significantly different between the two groups (Figure 2A, lower panel), indicating that AM251 had no effect on the intrinsic receptor kinase activity. Cells exposed to AM251 for 24 h resulted in a significant increase in phosphorylated Akt levels in response to EGF to 159.5 ± 15.4% of control ($P < 0.01$; Figure 2B).

Since increased EGFR activity has been associated with oncogenesis, a tumour cell invasion assay was performed using matrigel as the matrix barrier. PANC-1 cells treated with either EGF or AM251 exhibited comparable invasive behaviour, which was significantly greater than in untreated cells (Figure 3A). The number of invading cells almost doubled upon the addition of EGF to AM251-treated cells, suggesting that AM251 may prime PANC-1 cells to become hyper-responsive to EGF.

In addition to increased invasiveness, transformed cells often show reduced requirements for extracellular growth-promoting factors and are not restricted by cell–cell contact (Hanahan and Weinberg, 2000). This anchorage-independent growth, a hallmark of transformation, was measured using a soft agar colony formation assay. The treatment of PANC-1 cells with either EGF or AM251 yielded a similar number of colonies formed, which was significantly greater than in untreated cells (Figure 3B). Almost twice as many colonies were formed when the AM251-treated cells were stimulated with EGF. Four different starting densities (0.5, 1, 2 or 5 × 10^5 cells·mL^{-1}) were used, and while the data shown in Figure 3B represented the lowest density, the results were similar at all concentrations tested.

The proliferation of PANC-1 cells was assessed by flow cytometry analysis using propidium iodide staining to examine the cell cycle. In serum-starved cells, 11.3 ± 0.2% were in S phase (e.g. undergoing proliferation) and these numbers remained constant after 6 h of EGF treatment (Figure 3C); however, pretreatment with AM251 significantly increased the number of cells in S phase to 13.2 ± 0.7% ($P < 0.01$). When AM251-treated cells were subsequently incubated with EGF for 6 h, more than 17.5 ± 1.6% of cells were in S phase ($P < 0.001$ vs. AM251 alone). Under normal growth conditions (e.g. 10% FBS), 34.5% of cells were in S phase. An EGF time-course was performed from 0 to 24 h with the maximal effect seen after a 6 h treatment. All groups, including the untreated control group, showed 17.6–27.3% of cells in G2/M phase. These data show that the proliferative effect

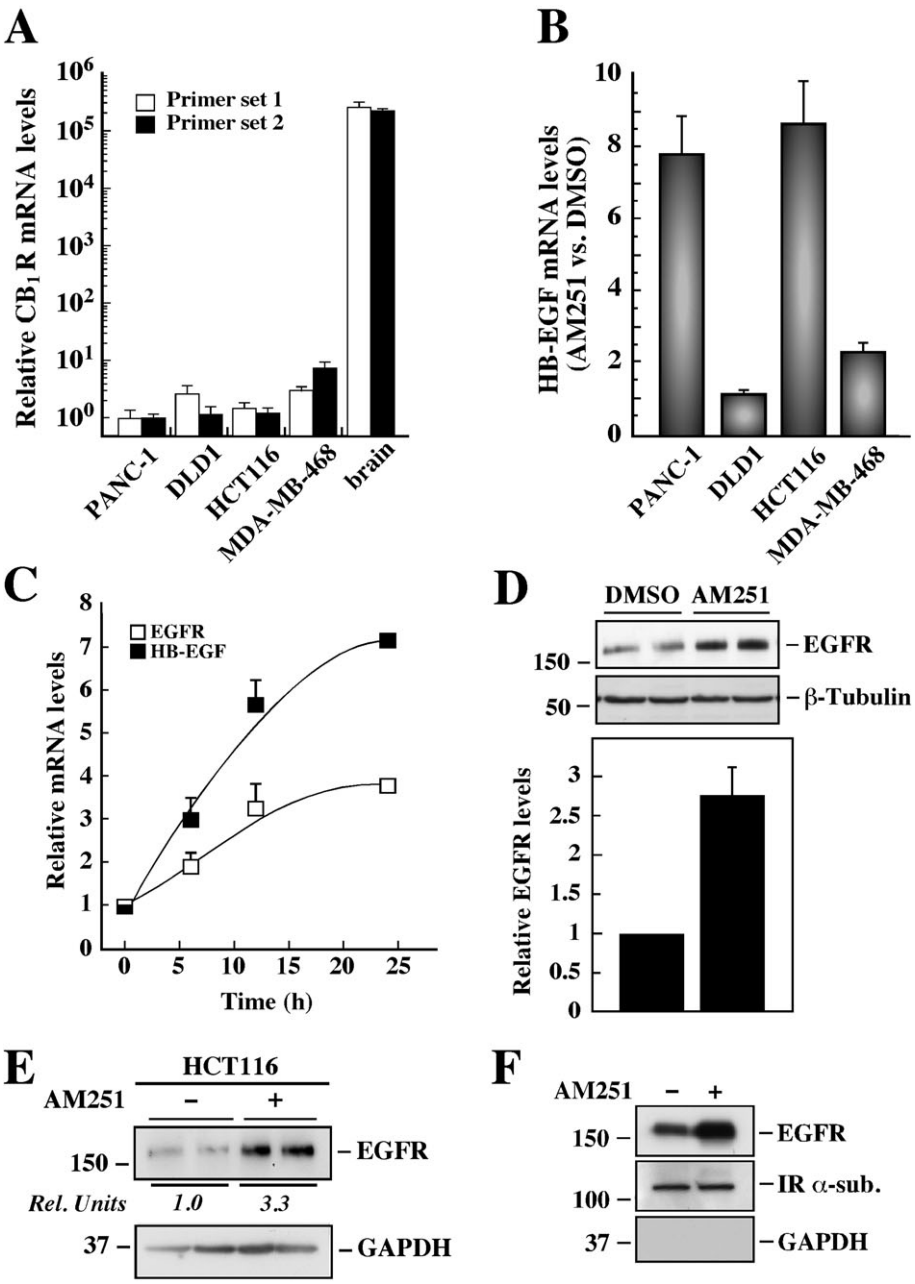

Figure 1

Cell type-specific induction of EGFR and HB-EGF gene expression by AM251. (A) The relative mRNA expression of cannabinoid 1 receptor (CB_1R) in a panel of cancer cell lines was assessed by quantitative PCR. Human brain total RNA was used as a positive control for CB_1R expression. Two sets of primers recognizing different isoforms of the CB_1R gene were analysed, and the values normalized to 18S mRNA expression. The data represent the average ± range of two independent experiments. (B) A panel of four cancer cell lines (PANC-1, DLD1, HCT116 and MDA-MD-468) were deprived of serum for 3 h followed by treatment with vehicle (DMSO) or AM251 (5 μM) for 24 h. The expression of HB-EGF mRNA was assessed by quantitative PCR, and the values were normalized to 18S mRNA levels. Shown is the ratio of HB-EGF mRNA in AM251 versus control group. The data represent the average ± range of two independent experiments. (C) PANC-1 cells were deprived of serum for 3 h followed by treatment with AM251 (5 μM) for the indicated periods of time. The relative mRNA expression of EGFR and HB-EGF was assessed by quantitative PCR, and the values were normalized to 18S mRNA levels. The data represent the average ± SD of two independent experiments. (D) Serum-starved PANC-1 cells were incubated with DMSO or AM251 (5 μM) for 24 h, after which total cell lysates were resolved by SDS–PAGE. Expression of EGFR was assessed by Western blot analysis, and reprobing the membrane for β-tubulin was used as a loading control. Columns represent the average ± SD of three independent experiments. $^{**}P < 0.01$ versus control. (E) HCT116 cells were treated as in (D), and Western blot analysis was performed using antibodies raised against EGFR, and GAPDH as a loading control. Rel. Units, the ratio of densitometry analysis of EGFR over GAPDH in the control group was arbitrarily set at 1.0. (F) PANC-1 cells were treated with either DMSO or AM251 (5 μM) for 24 h, and then subjected to biotinylation of cell surface proteins. Cellular proteins immobilized on NeutrAvidin agarose were eluted and subjected to Western blot analysis for the detection of EGFR, IR α-sub and GAPDH. (D–F) The migration of molecular mass markers (values in k Da) is shown on the left of immunoblots.

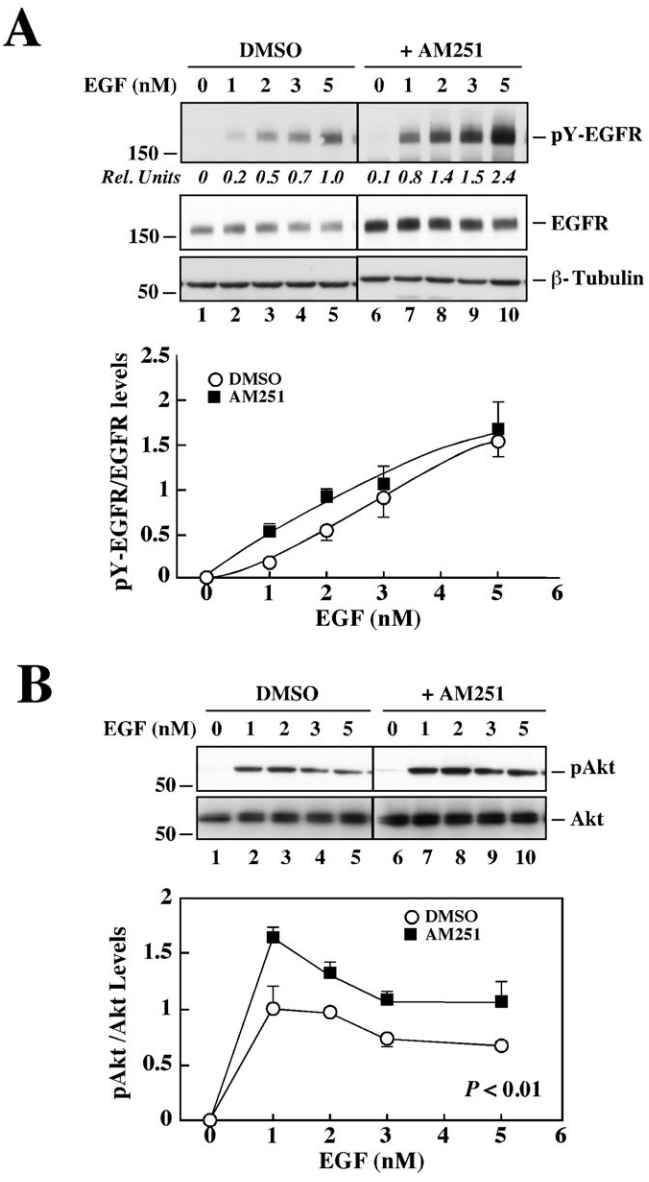

Figure 2

Dose-dependent EGF responsiveness in PANC-1 cells treated with AM251. (A) Serum-depleted PANC-1 cells were treated with vehicle (DMSO) or AM251 (5 μM) for 24 h followed by the addition of 0–5 nM recombinant EGF for 5 min. Total cell lysates were prepared and analysed by Western blot for total and tyrosine-phosphorylated EGFR levels. The blots were reprobed with anti-β-tubulin antibody as a loading control. The black line between the two sets of specimens indicates that treatment groups unrelated to the current study were deleted. Quantitative ratio of pY-EGFR to total EGFR is shown. (B) Western blot analysis of phosphoactive Akt and total Akt levels in PANC-1 cells. Quantitative ratio of pAkt/Akt is shown. The data represent the average ± range of two independent experiments. The migration of molecular mass markers (values in k Da) is shown on the left of immunoblots.

of EGF can be enhanced by AM251. Taken together, the results support the notion that AM251 treatment increases EGF responsiveness in PANC-1 cells partly through induction of endogenous EGFR expression.

AM251-induced expression of EGFR and its ligands through inhibition of oestrogen-related receptor α

As AM251 appeared to act by interacting with non-CB_1R cellular targets, it was imperative to identify the mediator(s) of AM251 signalling. In the light of earlier reports suggesting that DES also plays a role in EGFR regulation, we investigated the effects of DES on HB-EGF and EGFR expression in PANC-1 cells. Exposure to DES (20 μM) resulted in an up-regulation of EGFR and HB-EGF mRNA levels by 3.7 ± 0.5- and 38.2 ± 7.0-fold, respectively, versus control (Supporting Information Figure S3A). Western blot analysis was carried out, and the results showed a 1.5 ± 0.1-fold increase in EGFR expression in DES-treated cells versus control (Supporting Information Figure S3B).

Because PANC-1 cells are oestrogen receptor negative, it is likely that DES signals through orphan nuclear receptor ERRs, and consequently the effects of other ERR modulators were compared with AM251. Exposure of PANC-1 cells to the ERRα agonist biochanin A resulted in ~30% inhibition of HB-EGF mRNA levels, while the inverse agonist, XCT790, led to a 7.4 ± 0.5-fold increase in HB-EGF mRNA expression (Figure 4A). When cells were incubated with the ERRγ agonist, DY131, or the inverse agonist 4-OHT, HB-EGF mRNA levels were similar to the control group (Figure 4A). Given that ERRα and ERRγ are differentially expressed both in normal and tumour tissues (Gandhari *et al.*, 2010), it is tempting to speculate that some of the cellular processes involved in AM251 signalling may depend on the expression profile of ERR isoforms. Quantitative PCR analysis was performed in the panel of four tumour cell lines (PANC-1, DLD1, HCT116 and MDA-MB-468), and the data indicated that the mRNA ratio of 'ERRα/18S : ERRγ/18S' was the highest in the two AM251-responsive cell lines, PANC-1 and HCT116 (Figure 4B). A dose–response curve was then performed in PANC-1 cells using biochanin A, XCT790 and AM251 as a control. The XCT790 treatment mimicked the ability of AM251 to induce EGFR and HB-EGF mRNA expression, whereas both transcripts were decreased in the presence of biochanin A (Figure 4C). If one assumes that AM251 exerts its effects by inhibiting ERRα, then pretreatment of PANC-1 cells with the agonist biochanin A should interfere with subsequent response to AM251. Indeed, the AM251-induced increase in EGFR and HB-EGF mRNA expression (Figure 4D) and EGFR protein levels (Figure 4E) were significantly reduced by pre-incubating cells with biochanin A. Upon addition of XCT790, EGFR protein levels were increased 2.1- and 4.6-fold in PANC-1 and HCT116 cells, respectively ($P < 0.05$; Figure 4F, upper panel). Treatment with AM251 or XCT790 resulted in significant reduction in the levels of ERRα protein to 22 ± 5% of control (Figure 4E and F, middle panels, $P < 0.01$), whereas levels of ERRα mRNA were unaffected (data not shown). Exposure to DES also reduced the ERRα protein level, with an ED_{50} of 5 μM (data not shown).

ERRα has been reported to stimulate the expression of target genes, including pyruvate dehydrogenase kinase 4 (*PDK4*), osteopontin (*SPP1*) and PPARα (*PPARα*) (Vanacker *et al.*, 1998; Huss *et al.*, 2004; Wende *et al.*, 2005). Therefore, we sought to measure the endogenous mRNA levels for *PDK4*, *SPP1* and *PPARα* in response to AM251 and biochanin A. The

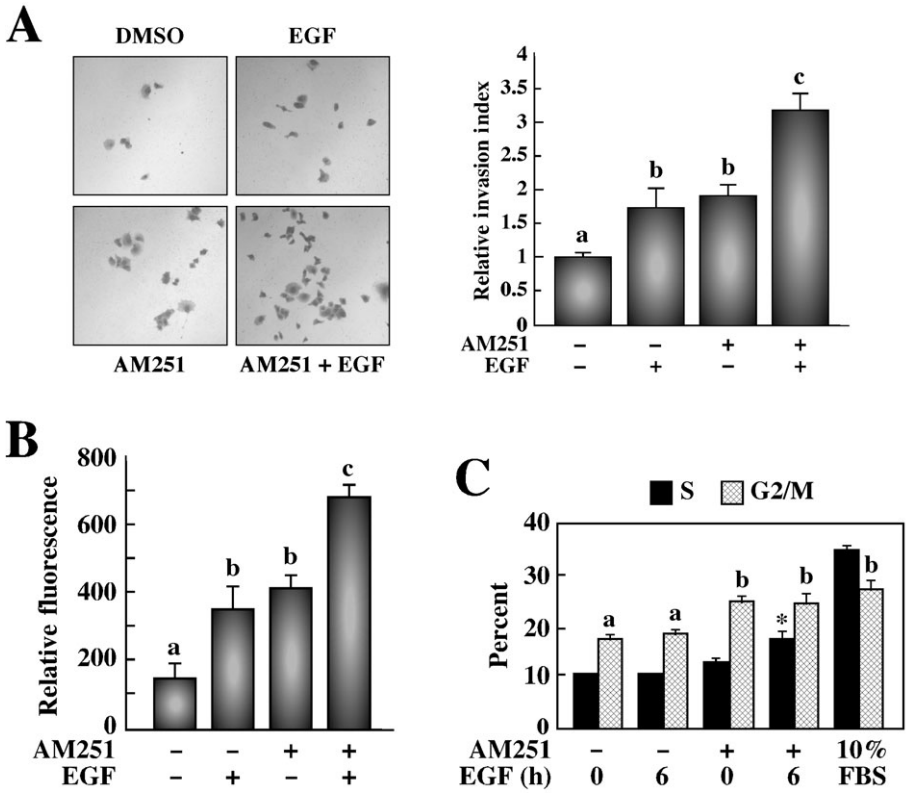

Figure 3

AM251 has enhancing effects on the response of EGF towards invasion, colony formation in soft agar and proliferation in PANC-1 cells. (A) Transwell migration chambers were used to determine invasive capacity of PANC-1 cells treated or not with AM251 (5 μM) for 24 h, followed by EGF (20 nM). After 72 h of invasion through matrigel, cells were stained with crystal violet, images were taken (left) and cells were counted (right). The data are representative of three independent experiments and is shown as the average ± SEM. Different letters (*a*, *b*, *c*) indicate significance of $P < 0.05$ among groups. (B) A soft agar colony formation assay was used to detect anchorage-independent growth of PANC-1 cells treated with AM251 for 24 h, followed by EGF (20 nM). After 7 days of growth in a semisolid agar media, cells were solubilized, lysed and detected by CyQuant GR Dye in a fluorescence plate reader. The histogram shows the relative fluorescence units from three independent experiments with a starting density of 0.5×10^5 cells·mL^{-1}. The data are shown as the average ± SEM. (C) Propidium iodide staining was used to determine DNA cell cycle analysis by flow cytometry. The columns represent the % of PANC-1 cells in the S and G2/M stages of the cell cycle after treatment with AM251 (5 μM) for 24 h and EGF (20 nM) for 6 h. Cells left untreated in complete media (10% FBS) were used as a control. The data represent the average ± SD ($n = 3$). Different letters (*a*, *b*) indicate significance of $P < 0.01$ among groups. *$P < 0.001$ versus AM251-treated cells.

results indicate that treatment of PANC-1 cells with the ERRα agonist, biochanin A, induced a 2.9 ± 0.2-, 2.0 ± 0.3- and 1.9 ± 0.1-fold increase in *PDK4*, *SPP1* and *PPARα* mRNA levels, respectively, whereas a 40–50% reduction in gene expression was observed with AM251 (Figure 4G). In some instances, biochanin A pretreatment rendered cells refractory to subsequent AM251 signalling. It should be noted that these actions of AM251 were reproduced by XCT790 (data not shown).

Preliminary experiments demonstrated that transfection of PANC-1 cells with the *ERRα* siRNA led to a 90% knock-down in ERRα protein expression compared with the negative, non-silencing control (data not shown). Levels of GAPDH were unaffected, indicating a low probability of non-specific silencing effects. The siRNA-mediated knock-down of *ERRα* in PANC-1 cells led to constitutive induction in EGFR and HB-EGF mRNA levels, and treatment with AM251 or XCT790 had no further stimulating effect (Figure 5A). To confirm that the biological responses of AM251 and XCT790 occurred through ERRα, cell cycle analysis was performed using control and *ERRα* siRNA-transfected PANC-1 (Figure 5B, upper panel) and HCT116 (Figure 5B, lower panel) cells. When the control, non-targeting siRNA was used, subsequent exposure to AM251 or XCT790 resulted in a doubling of the number of cells in the S phase. However, this increase did not occur after ERRα gene knock-down due largely to the higher percentage of cells already in the S phase (15.5 vs 8.5% in PANC-1 cells, and 29.5 vs 16.5% in HCT116 cells after transfection with *ERRα* siRNA vs. control siRNA, respectively) (Figure 5B).

Direct interaction of AM251 to the immobilized LBD of ERRα

Purified recombinant His-tagged ERRα LBD was immobilized on a chromatographic support to characterize the binding properties of AM251 using frontal displacement chromatography. DES was recently shown to bind to the ERRα LBD column with a K_d of 929 nM (Sanghvi *et al.*, 2010). Here, the same column that was used to calculate the binding affinity

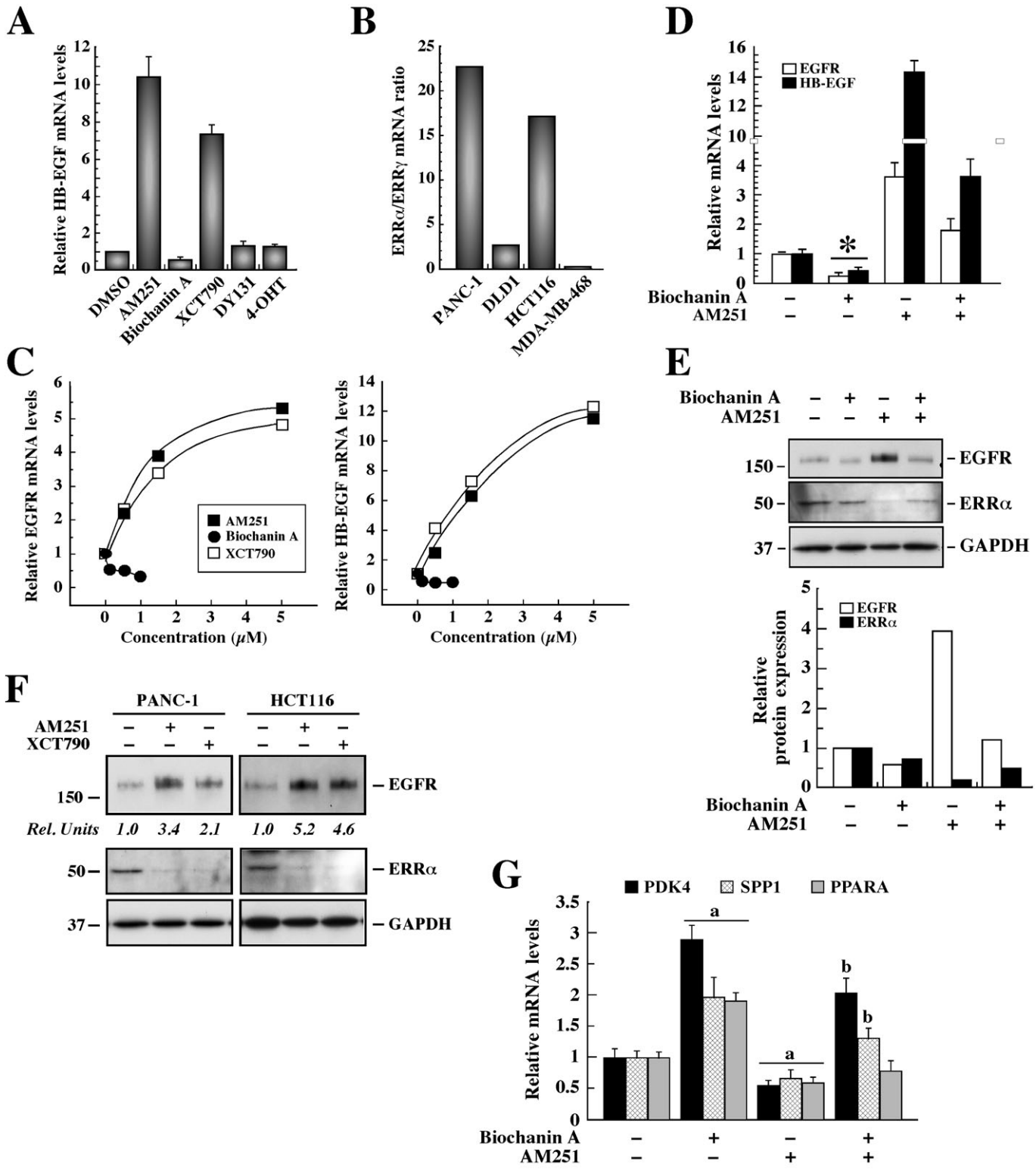

of AM251 was also employed to determine the binding properties of biochanin A. Frontal displacement chromatography using DES as the ERRα marker ligand indicated that biochanin A bound to the immobilized ERRα LBD column with a binding affinity, K_d, of 64 nM (Figure 6A). We then examined the effect of serial mobile phase concentrations of the displacer ligand AM251 on the chromatographic retention of DES, and found that AM251 elicited a dose-dependent elution of DES, with a K_d of 419 ± 260 nM (r^2 = 0.900; Figure 6B). In addition, 4-OHT, a known ERRγ antagonist

Figure 4

Drug-induced expression of EGFR and HB-EGF through destabilization of ERRα. (A) PANC-1 cells were deprived of serum for 3 h followed by treatment with AM251 (5 μM), biochanin A (100 nM), XCT790 (1.5 μM), DY131 (100 nM) or 4-OHT (1 μM) for 24 h. The relative HB-EGF mRNA level was assessed by quantitative PCR, and the values were normalized to 18S mRNA. The data represent the average ± range of two independent experiments. (B) ERRα and ERRγ mRNA expression was examined by quantitative PCR in a panel of cancer cell lines. The values were normalized to 18S mRNA, and the 'ERRα/18S : ERRγ/18 S' mRNA ratio was calculated. The data represent the average ± range of two independent experiments. (C) PANC-1 cells were deprived of serum for 3 h followed by treatment with AM251 (0–5 μM), biochanin A (0–1 μM) and XCT790 (0–5 μM) for 24 h. Quantitative PCR analysis of EGFR (top) and HB-EGF (bottom) mRNA expression was performed, and the values were normalized to 18S mRNA levels. (D) Serum-starved PANC-1 cells were pretreated or not with biochanin A (1 μM) for 1 h followed by the addition of vehicle or AM251 (5 μM) for 24 h. The relative HB-EGF and EGFR mRNA levels were assessed by quantitative PCR, and the values were normalized to 18S mRNA. The data represent the average ± SEM of three independent experiments. *$P < 0.01$ versus DMSO control. (E) PANC-1 cells were treated as in (D) and subjected to Western blot analysis for EGFR expression levels. The blot was reprobed with anti-GAPDH antibody as a loading control. The migration of molecular mass markers (values in k Da) is shown on the left of immunoblots. (F) PANC-1 and HCT116 cells were treated with vehicle, AM251 (5 μM) or XCT790 (1.5 μM) for 24 h. Total cell lysates were analysed by Western blot for EGFR, ERRα and GAPDH as a loading control. (E and F) Rel. Units, densitometry analysis of EGFR expression levels relative to vehicle-treated controls. The data represent the average fold stimulation from three independent experiments. (G) Quantitative PCR analysis of *PDK4*, *SPP1* and *PPARα* mRNA was performed with the samples described in (D), and the values were normalized to 18S mRNA. The data represent the average ± SD ($n = 3$). Comparable results were obtained in a second independent experiment. *a*, $P \leq 0.05$ versus control; *b*, $P < 0.01$ versus AM251-treated cells.

with no known affinity for the ERRα (Coward *et al.*, 2001), did not have any affinity for the ERRα LBD column (data not shown).

Discussion

This study establishes a potentially useful 'off-target' action of AM251, a compound reported to be relatively selective as a CB_1R inverse agonist. Using genetic, biochemical and pharmacological approaches, we showed that the transcriptional induction of EGFR and its cognate ligands is not related to modulation of CB_1R. Instead, AM251 functions as an inverse agonist of ERRα, and like the synthetic oestrogen DES and the classical inverse agonist XCT790, induces proteolytic degradation of the orphan nuclear receptor. The notion that AM251 signals through ERRα inhibition is supported by the finding that the ability of AM251 to induce EGFR expression and biological responses was blocked by the addition of the ERRα agonist, biochanin A, or the silencing of ERRα.

A principal goal of this study was to investigate CB_1R-independent signalling of AM251 in a panel of human cancer cell lines that express low to undetectable CB_1R levels. Exposure of PANC-1 cells to AM251, but not related compounds, such as WIN 55212-2 and AM630, induced EGFR mRNA and protein expression, but not that of the IGF-1 receptor. HB-EGF and betacellulin are two cognate EGFR ligands whose mRNA levels were also up-regulated by AM251. Whereas the colon cancer cell line HCT116 responded to AM251 with increased expression of EGFR and HB-EGF, DLD1 and MDA-MB-468 cells were unresponsive when compared to vehicle-treated controls. We suspect this observation may reflect differences in the expression and/or functionality of the molecular targets of AM251 between cancer cell lines. From these results, it became important to establish the mechanism of AM251 signalling.

Despite being negative for oestrogen receptor α (Abe *et al.*, 2000; Guo *et al.*, 2004), PANC-1 cells are responsive to the anti-proliferative effects of the phytoestrogen daidzein (Guo *et al.*, 2004), a known ERRα agonist (Ariazi and Jordan, 2006). It is well recognized that a high expression of ERRα in tumours of various origins is associated with bad prognosis and higher EGFR signalling (Ariazi *et al.*, 2002; Suzuki *et al.*, 2004; Cavallini *et al.*, 2005; Sun *et al.*, 2005). Inhibition of ERRα expression decreases cell proliferation and migration in breast cancer (Stein and McDonnell, 2006). In contrast, exposure to the ERRα agonist, biochanin A, results in growth inhibition of human prostate cancer cells (Peterson and Barnes, 1993). Here, we showed that ERRα has intrinsic anti-proliferative activity in PANC-1 and HCT116 cells (Figure 5B). Interestingly, exposure to the phytoestrogens genistein, daidzein and biochanin A decreases EGFR expression in human osteosarcoma cells (Salvatori *et al.*, 2009), but not in porcine skeletal muscle cell cultures or HT-29 human colon cancer cells (Kim *et al.*, 2005b; Kalbe *et al.*, 2008). These conflicting results are consistent with the view that the effects of ERRα on proliferation, migration and invasiveness may vary with cell type, and may depend on the formation of appropriate levels of ERRα homo- and/or heterodimerization with interacting partners. Our quantitative PCR experiments using ERR isoform-specific primers suggest the presence of both ERRα and ERRγ in PANC-1 cells, with a 22-fold higher expression level of the former orphan nuclear receptor. It is interesting that in addition to PANC-1 cells, only the HCT116 cell line displays a high (16-fold) ERRα/ERRγ ratio. Protein dimerization modulates ERR transcriptional activity, and, although being able to bind DNA as a monomer, ERRα can heterodimerize with ERRγ, thereby altering the binding and regulatory activities of both nuclear receptors (Huppunen and Aarnisalo, 2004). Therefore, formation of ERRα–ERRγ heterodimers may well direct a transcriptional profile distinct from that of ERRα homodimers, such that graded expression of ERRγ may convert ERRα from a repressor to a transcriptional activator in some cell types.

Our data show that the AM251-induced increase in HB-EGF and EGFR expression depends on ERRα status. A similar increase in gene expression was obtained using DES and the highly specific inverse agonist, XCT790, whereas it was blocked by the ERRα activator biochanin A. Moreover, these modulators of ERRα transcriptional activity were found to reciprocally regulate the expression of three ERRα targets: *PDK4*, *SPP1* and *PPARα* (Figure 4G). Several transcription

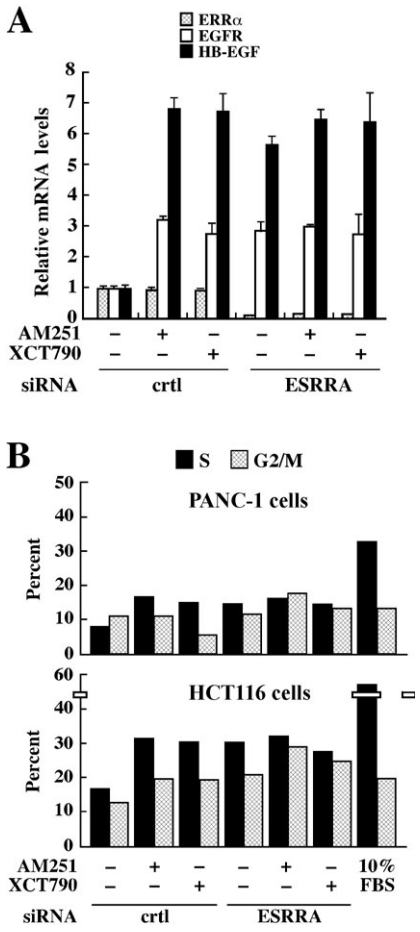

Figure 5

Effect of ERRα silencing on cell cycle in the presence of AM251 or XCT790. (A) PANC-1 cells were transfected with a control, non-targeting siRNA or with *ERRα* siRNA for 24 h. Cells were deprived of serum for 3 h, and then treated with DMSO, AM251 (5 μM) or XCT790 (1.5 μM) for 24 h. The relative HB-EGF and EGFR mRNA levels were assessed by quantitative PCR, and the values were normalized to 18S mRNA. The data represent the average ± range of two independent experiments. (B) Control and *ERRα*-transfected (ESRRA) PANC-1 (upper) and HCT116 (lower) cells were exposed to AM251 (5 μM) or XCT790 (1.5 μM) for 24 h, and then processed for propidium iodide staining. The columns represent the % of cells in the S and G2/M stages of the cell cycle. Cells left in complete media (10% FBS) were used as a control. Shown is the average of two dishes per treatment group. Similar results were obtained in a second independent experiment.

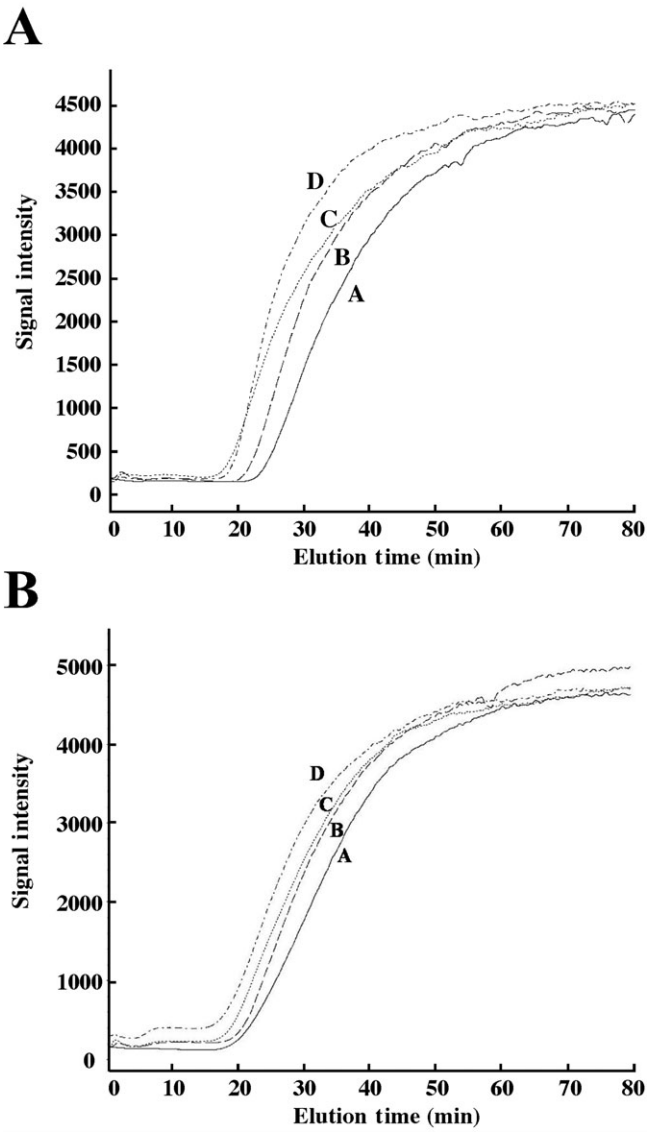

Figure 6

Binding affinity of biochanin A and AM251 for the immobilized ERRα LBD. Chromatographic traces obtained for DES (0.25 μM) on the ERRα LBD column displaced with varying concentrations of biochanin A (in μM; A: 0.1; B: 0.25; C: 0.5; D: 0.75) (A) or AM251 (in μM; A: 0.25; B: 0.5; C: 1; D: 2) (B).

factors and nuclear receptors, including ERRα, are co-activated by PPAR co-activator-1α (PGC-1α). Specifically, induction of genes encoding mitochondrial proteins, vascular endothelial growth factor and glucokinase requires a functional PGC-1α/ERRα interaction (Schreiber *et al.*, 2004; Stein *et al.*, 2009; Zhu *et al.*, 2010), and the co-operative interaction of Bcl3 with PGC-1α also results in ERRα activation (Yang *et al.*, 2009). Conversely, recruitment of the co-repressor RIP140/NRIP1 (receptor-interacting protein 140) and protein inhibitor of activated signal transducer and activator of transcription-γ (PIAS4) prevents the transcription of ERRα target genes (Hallberg *et al.*, 2008; Tremblay *et al.*, 2008). In our experiment, exposure to XCT790 resulted in a significant increase in EGFR/HB-EGF gene transcription to levels comparable to AM251. XCT790 disrupts the interaction between ERRα and PGC-1α, but has no effect on either the oestrogen receptors or other ERR isoforms (Busch *et al.*, 2004; Willy *et al.*, 2004). Therefore, it is possible that AM251 could interfere with ERRα transcriptional activation by altering the recruitment of nuclear co-regulatory molecules and other DNA-binding proteins to ERRα at the target gene promoter region.

A key finding of our study is that ERRα protein levels were selectively reduced in PANC-1 cells treated either with

AM251, DES or XCT790, but these compounds had no effect on PGC-1α expression or ERRα mRNA levels. XCT790 has been recently reported to promote the degradation of ERRα protein in MCF7 cells without loss of the corresponding mRNA (Lanvin *et al.*, 2007). Therefore, it is unlikely that transcriptional (auto)-regulation of ERRα is involved in AM251 signalling. We can only speculate on the basic mechanisms underlying this inducible ERRα protein loss. Recent studies have shown the importance of the phosphorylation-dependent ubiquitination process in the degradation of numerous signalling proteins (reviewed in Hunter, 2007). Although we did not measure the extent of ERRα phosphorylation, this nuclear receptor is phosphorylated on several residues, and data suggest a positive effect of phosphorylation on sumoylation of ERRα through the rapid recruitment of PIAS4, a small ubiquitin-related modifier E3 ligase (Vu *et al.*, 2007; Tremblay *et al.*, 2008).

The notion that AM251 and its clinical analogue, rimonabant, elicit CB_1R-independent actions has long been debated because several studies have reported that administration of these compounds was able to promote off-target effects. In fact, the orphan GPCR, GPR55, has been assigned as a candidate cannabinoid receptor in HEK293 transfected cells (Ryberg *et al.*, 2007; Lauckner *et al.*, 2008; Yin *et al.*, 2009), although such functionality of endogenously expressed GPR55 is contested (Oka *et al.*, 2007; 2009). Despite the presence of GPR55 in the murine microglial cell line BV-2, rimonabant and most of the cannabinoids tested did not elicit an agonistic response (Eldeeb *et al.*, 2009). It has also been shown that endocannabinoids bind to the vanilloid receptor 1 (VR1) (Smart *et al.*, 2000; Ralevic *et al.*, 2001) in a cell type- and tissue-dependent manner. Expression of VR1 is significantly up-regulated in human pancreatic cancer and chronic pancreatitis, and the vanilloid analogue, resiniferatoxin, induces apoptosis in pancreatic cancer cells (Hartel *et al.*, 2006). Studies reporting functional cross-talk between VR1 and CB_1R have demonstrated that activation of either or both receptors mediated the cell death of dopaminergic neurons (Kim *et al.*, 2005a). Conversely, an increase in neurogenesis by rimonabant and AM251 may occur via CB_1R-independent signalling, as VR1 activation appears to be an essential component of enhanced neurogenesis by rimonabant in mice with targeted deletion of CB_1Rs (Jin *et al.*, 2004). The present study provides experimental evidence that the cellular actions of AM251 involves ERRα, showing not only that AM251 interacts directly with ERRα LBD *in vitro*, but also that blockade of ERRα signalling with DES, XCT790 or gene knock-down by siRNA elicits an increase in gene expression that is reminiscent of the situation with AM251. The possibility still exists that AM251 is hitting a target other than ERRα that is involved in the regulation of cell cycle and migration. However, a direct comparison of the effect of XCT790 with AM251 on the cell cycle parameters was performed in two different cancer cell lines after the silencing of ERRα. The results showed the critical role of ERRα turnover in AM251-mediated signalling. From our data we cannot definitely determine what other cellular targets, if any, are regulating EGFR expression and downstream signalling in response to AM251, but future studies should examine the role of both GPR55 and VR1 in the control of tumour cell progression.

Compounds, such as AM251 and rimonabant, contain halogen group substitutions by chloride, as well as a phenolic moiety, two characteristics that are shared with the organochlorine pesticides toxaphene and chlordane, which are known ERRα inhibitors (Ariazi and Jordan, 2006). In this study, using ERRα LBD immobilized on a chromatographic support, we found that AM251 displaces the synthetic, non-steroidal oestrogen drug DES with a K_d value in the 400 nM range. Accordingly, these properties could have a profound effect not only in endocrine disruption, but also in tumour cell survival in certain cancers as a consequence of exposure to these compounds. Our preliminary study *in vitro* has shown that exposure of PANC-1 cells to AM251 elicits a new mesenchymal-like phenotype with loss in lineage-specific markers, such as E-cadherin (J.L. Fiori and M. Bernier, unpubl. obs.), indicating the disturbance of important regulatory mechanisms thought to play an essential role in embryonic development and cancer progression (Schmalhofer *et al.*, 2009; Vandewalle *et al.*, 2009).

In summary, this is the first study to demonstrate that AM251 stimulates EGFR expression and signalling not through CB_1R inhibition, but through binding to and destabilization of the orphan nuclear receptor ERRα. It also underscores that the generality of this observation will have to be established using normal cells and human tumour cell lines from different origins. A thorough investigation of the health hazard of AM251 and related classes of compounds as potential endocrine-disrupting chemicals and cancer-inducing agents is warranted. This study has potentially important implications for the AM251 clinical analogue rimonabant, as rimonabant had been used clinically to decrease food intake (Van Gaal *et al.*, 2005). Our study provides a rationale to investigate whether other cannabinoid receptor inverse agonists also bind to and cause degradation of ERRα. It is tempting to speculate that this class of compounds could be exerting their inhibitory effects against obesity, at least in part, through ERRα. In this regard, ERRα knock-out mice show defects in fatty acid metabolism and are resistant to diet-induced obesity (Luo *et al.*, 2003).

Acknowledgements

We thank Drs Robert P. Wersto for expert advice on flow cytometry analysis and Irving W. Wainer for critical reading of the manuscript. We would also like to thank Sutapa Kole for her technical assistance and Jade Scheers in the Research Resources Branch at the NIA for her technical assistance with the flow cytometry, which includes sample preparation, flow acquisition and cell cycle analysis. This research was supported entirely by the Intramural Research Program of the NIH, NIA.

Conflict of interest

None to declare.

References

Abe M, Yamashita J, Ogawa M (2000). Medroxyprogesterone acetate inhibits human pancreatic carcinoma cell growth by inducing apoptosis in association with Bcl-2 phosphorylation. Cancer 88: 2000–2009.

Ariazi EA, Jordan VC (2006). Estrogen-related receptors as emerging targets in cancer and metabolic disorders. Curr Top Med Chem 6: 203–215.

Ariazi EA, Clark GM, Mertz JE (2002). Estrogen-related receptor α and estrogen-related receptor γ associate with unfavorable and favorable biomarkers, respectively, in human breast cancer. Cancer Res 62: 6510–6518.

Bátkai S, Pacher P, Járai Z, Wagner JA, Kunos G (2004). Cannabinoid antagonist SR-141716 inhibits endotoxic hypotension by a cardiac mechanism not involving CB1 or CB2 receptors. Am J Physiol Heart Circ Physiol 287: H595–H600.

Bhola NE, Grandis JR (2008). Crosstalk between G-protein-coupled receptors and epidermal growth factor receptor in cancer. Front Biosci 13: 1857–1865.

Bukoski RD, Bátkai S, Járai Z, Wang Y, Offertaler L, Jackson WF *et al.* (2002). CB(1) receptor antagonist SR141716A inhibits Ca(2+)-induced relaxation in CB(1) receptor-deficient mice. Hypertension 39: 251–257.

Busch BB, Stevens WC Jr, Martin R, Ordentlich P, Zhou S, Sapp DW *et al.* (2004). Identification of a selective inverse agonist for the orphan nuclear receptor estrogen-related receptor α. J Med Chem 47: 5593–5596.

Caffarel MM, Sarrió D, Palacios J, Guzmán M, Sánchez C (2006). Delta9-tetrahydrocannabinol inhibits cell cycle progression in human breast cancer cells through Cdc2 regulation. Cancer Res 66: 6615–6621.

Cavallini A, Notarnicola M, Giannini R, Montemurro S, Lorusso D, Visconti A *et al.* (2005). Oestrogen receptor-related receptor alpha (ERRα) and oestrogen receptors (ERα and ERβ) exhibit different gene expression in human colorectal tumour progression. Eur J Cancer 41: 1487–1494.

Coward P, Lee D, Hull MV, Lehmann J (2001). 4-Hydroxytamoxifen binds to and deactivates the estrogen-related receptor γ. Proc Natl Acad Sci USA 98: 8880–8884.

Di S, Malcher-Lopes R, Marcheselli VL, Bazan NG, Tasker JG (2005). Rapid glucocorticoid-mediated endocannabinoid release and opposing regulation of glutamate and gamma-aminobutyric acid inputs to hypothalamic magnocellular neurons. Endocrinology 146: 4292–4301.

Eldeeb K, Alexander S, Pritchard D, Kendall D (2009). LPI-evoked increases in intracellular calcium increases in microglial cells in culture. *19th annual symposium of the International Cannabinoid Research Society*, ICRS, St. Charles, IL, p. 21.

Gandhari MK, Frazier CR, Hartenstein JS, Cloix JF, Bernier M, Wainer IW (2010). Identification and characterization of estrogen receptor-related receptor α and γ in human glioma and astrocytoma cells. Mol Cell Endocrinol 315: 314–318.

Greulich H, Chen TH, Feng W, Jänne PA, Alvarez JV, Zappaterra M *et al.* (2005). Oncogenic transformation by inhibitor-sensitive and -resistant EGFR mutants. PLoS Med 2: e313.

Guo JM, Xiao BX, Dai DJ, Liu Q, Ma HH (2004). Effects of daidzein on estrogen-receptor-positive and negative pancreatic cancer cells *in vitro*. World J Gastroenterol 10: 860–863.

Hallberg M, Morganstein DL, Kiskinis E, Shah K, Kralli A, Dilworth SM *et al.* (2008). A functional interaction between RIP140 and PGC-1α regulates the expression of the lipid droplet protein CIDEA. Mol Cell Biol 28: 6785–6795.

Hanahan D, Weinberg RA (2000). The hallmarks of cancer. Cell 100: 57–70.

Hart S, Fischer OM, Ullrich A (2004). Cannabinoids induce cancer cell proliferation via tumor necrosis factor alpha-converting enzyme (TACE/ADAM17)-mediated transactivation of the epidermal growth factor receptor. Cancer Res 64: 1943–1950.

Hartel M, di Mola FF, Selvaggi F, Mascetta G, Wente MN, Felix K *et al.* (2006). Vanilloids in pancreatic cancer: potential for chemotherapy and pain management. Gut 55: 519–528.

Herkenham M, Lynn AB, Johnson MR, Melvin LS, de Costa BR, Rice KC (1991). Characterization and localization of cannabinoid receptors in rat brain: a quantitative *in vitro* autoradiographic study. J Neurosci 11: 563–583.

Hunter T (2007). The age of crosstalk: phosphorylation, ubiquitination, and beyond. Mol Cell 28: 730–738.

Huppunen J, Aarnisalo P (2004). Dimerization modulates the activity of the orphan nuclear receptor ERRγ. Biochem Biophys Res Commun 314: 964–970.

Huss JM, Torra IP, Staels B, Giguère V, Kelly DP (2004). Estrogen-related receptor alpha directs peroxisome proliferator-activated receptor alpha signaling in the transcriptional control of energy metabolism in cardiac and skeletal muscle. Mol Cell Biol 24: 9079–9091.

Iguchi T, Edery M, Tasi PS, Ozawa S, Sato T, Bern HA (1993). Epidermal growth factor receptor levels in reproductive organs of female mice exposed neonatally to diethylstilbestrol. Proc Soc Exp Biol Med 204: 110–116.

Jin K, Xie L, Kim SH, Parmentier-Batteur S, Sun Y, Mao XO *et al.* (2004). Defective adult neurogenesis in CB1 cannabinoid receptor knockout mice. Mol Pharmacol 66: 204–208.

Kalbe C, Mau M, Rehfeldt C (2008). Developmental changes and the impact of isoflavones on mRNA expression of IGF-I receptor, EGF receptor and related growth factors in porcine skeletal muscle cell cultures. Growth Horm IGF Res 18: 424–433.

Kim SR, Lee DY, Chung ES, Oh UT, Kim SU, Jin BK (2005a). Transient receptor potential vanilloid subtype 1 mediates cell death of mesencephalic dopaminergic neurons *in vivo* and *in vitro*. J Neurosci 25: 662–671.

Kim EJ, Shin HK, Park JH (2005b). Genistein inhibits insulin-like growth factor-I receptor signaling in HT-29 human colon cancer cells: a possible mechanism of the growth inhibitory effect of genistein. J Med Food 8: 431–438.

Lanvin O, Bianco S, Kersual N, Chalbos D, Vanacker JM (2007). Potentiation of ICI182,780 (fulvestrant)-induced estrogen receptor-α degradation by the estrogen receptor-related receptor-α inverse agonist XCT790. J Biol Chem 282: 28328–28334.

Lauckner JE, Jensen JB, Chen HY, Lu HC, Hille B, Mackie K (2008). GPR55 is a cannabinoid receptor that increases intracellular calcium and inhibits M current. Proc Natl Acad Sci USA 105: 2699–2704.

Luo J, Sladek R, Carrier J, Bader JA, Richard D, Giguère V (2003). Reduced fat mass in mice lacking orphan nuclear receptor estrogen-related receptor alpha. Mol Cell Biol 23: 7947–7956.

Maa MC, Leu TH, McCarley DJ, Schatzman RC, Parsons SJ (1995). Potentiation of epidermal growth factor receptor-mediated oncogenesis by c-Src: implications for the etiology of multiple human cancers. Proc Natl Acad Sci USA 92: 6981–6985.

Marszałł MP, Moaddel R, Kole S, Gandhari M, Bernier M, Wainer IW (2008). Ligand and protein fishing with heat shock protein 90 coated magnetic beads. Anal Chem 80: 7571–7575.

Matsuda LA, Bonner TI, Lolait SJ (1993). Localization of cannabinoid receptor mRNA in rat brain. J Comp Neurol 327: 535–550.

Melck D, De Petrocellis L, Orlando P, Bisogno T, Laezza C, Bifulco M *et al*. (2000). Suppression of nerve growth factor Trk receptors and prolactin receptors by endocannabinoids leads to inhibition of human breast and prostate cancer cell proliferation. Endocrinology 141: 118–126.

Mimeault M, Pommery N, Wattez N, Bailly C, Hénichart JP (2003). Anti-proliferative and apoptotic effects of anandamide in human prostatic cancer cell lines: implication of epidermal growth factor receptor down-regulation and ceramide production. Prostate 56: 1–12.

Moaddel R, Wainer IW (2009). The preparation and development of cellular membrane affinity chromatography columns. Nat Protoc 4: 197–205.

Murphy LO, Cluck MW, Lovas S, Otvös F, Murphy RF, Schally AV *et al*. (2001). Pancreatic cancer cells require an EGF receptor-mediated autocrine pathway for proliferation in serum-free conditions. Br J Cancer 84: 926–935.

Nicholson RI, Gee JM, Harper ME (2001). EGFR and cancer prognosis. Eur J Cancer 37: S9–S15.

Oka S, Nakajima K, Yamashita A, Kishimoto S, Sugiura T (2007). Identification of GPR55 as a lysophosphatidylinositol receptor. Biochem Biophys Res Commun 362: 928–934.

Oka S, Toshida T, Maruyama K, Nakajima K, Yamashita A, Sugiura T (2009). 2-Arachidonoyl-sn-glycero-3-phosphoinositol: a possible natural ligand for GPR55. J Biochem 145: 13–20.

Paolillo M, Schinelli S (2008). Therapeutic targeting of G-protein coupled receptor-mediated epidermal growth factor receptor transactivation in human glioma brain tumors. Mini Rev Med Chem 8: 1418–1428.

Patsos HA, Hicks DJ, Dobson RR, Greenhough A, Woodman N, Lane JD *et al*. (2005). The endogenous cannabinoid, anandamide, induces cell death in colorectal carcinoma cells: a possible role for cyclooxygenase 2. Gut 54: 1741–1750.

Peterson G, Barnes S (1993). Genistein and biochanin A inhibit the growth of human prostate cancer cells but not epidermal growth factor receptor tyrosine autophosphorylation. Prostate 22: 335–345.

Ralevic V, Kendall DA, Jerman JC, Middlemiss DN, Smart D (2001). Cannabinoid activation of recombinant and endogenous vanilloid receptors. Eur J Pharmacol 424: 211–219.

Ramer R, Brune K, Pahl A, Hinz B (2001). *R*(+)-methanandamide induces cyclooxygenase-2 expression in human neuroglioma cells via a non-cannabinoid receptor-mediated mechanism. Biochem Biophys Res Commun 286: 1144–1152.

Rodgers RJ, Evans PM, Murphy A (2005). Anxiogenic profile of AM-251, a selective cannabinoid CB1 receptor antagonist, in plus-maze-naïve and plus-maze-experienced mice. Behav Pharmacol 16: 405–413.

Ruiz L, Miguel A, Díaz-Laviada I (1999). Delta9-tetrahydrocannabinol induces apoptosis in human prostate PC-3 cells via a receptor-independent mechanism. FEBS Lett 458: 400–404.

Ryberg E, Larsson N, Sjögren S, Hjorth S, Hermansson NO, Leonova J *et al*. (2007). The orphan receptor GPR55 is a novel cannabinoid receptor. Br J Pharmacol 152: 1092–1101.

Salvatori L, Pallante P, Ravenna L, Chinzari P, Frati L, Russo MA *et al*. (2003). Oestrogens and selective oestrogen receptor (ER) modulators regulate EGF receptor gene expression through human ER α and β subtypes via an Sp1 site. Oncogene 22: 4875–4881.

Salvatori L, Caporuscio F, Coroniti G, Starace G, Frati L, Russo MA *et al*. (2009). Down-regulation of epidermal growth factor receptor induced by estrogens and phytoestrogens promotes the differentiation of U2OS human osteosarcoma cells. J Cell Physiol 220: 35–44.

Sanghvi M, Moaddel R, Frazier C, Wainer IW (2010). Synthesis and characterization of liquid chromatographic columns containing the immobilized ligand-binding domain of the estrogen related receptor α and estrogen related receptor γ. J Pharm Biomed Anal 53: 777–780.

Sarfaraz S, Afaq F, Adhami VM, Mukhtar H (2005). Cannabinoid receptor as a novel target for the treatment of prostate cancer. Cancer Res 65: 1635–1641.

Schmalhofer O, Brabletz S, Brabletz T (2009). E-cadherin, beta-catenin, and ZEB1 in malignant progression of cancer. Cancer Metastasis Rev 28: 151–166.

Schreiber SN, Emter R, Hock MB, Knutti D, Cardenas J, Podvinec M *et al*. (2004). The estrogen-related receptor alpha (ERRα) functions in PPARγ coactivator 1α (PGC-1α)-induced mitochondrial biogenesis. Proc Natl Acad Sci USA 101: 6472–6477.

Smart D, Gunthorpe MJ, Jerman JC, Nasir S, Gray J, Muir AI *et al*. (2000). The endogenous lipid anandamide is a full agonist at the human vanilloid receptor (hVR1). Br J Pharmacol 129: 227–230.

Stein RA, McDonnell DP (2006). Estrogen-related receptor alpha as a therapeutic target in cancer. Endocr Relat Cancer 13: S25–S32.

Stein RA, Gaillard S, McDonnell DP (2009). Estrogen-related receptor alpha induces the expression of vascular endothelial growth factor in breast cancer cells. J Steroid Biochem Mol Biol 114: 106–112.

Sun P, Sehouli J, Denkert C, Mustea A, Könsgen D, Koch I *et al*. (2005). Expression of estrogen receptor-related receptors, a subfamily of orphan nuclear receptors, as new tumor biomarkers in ovarian cancer cells. J Mol Med 83: 457–467.

Suzuki T, Miki Y, Moriya T, Shimada N, Ishida T, Hirakawa H *et al*. (2004). Estrogen-related receptor α in human breast carcinoma as a potent prognostic factor. Cancer Res 64: 4670–4676.

Tremblay GB, Bergeron D, Giguère V (2001a). 4-Hydroxytamoxifen is an isoform-specific inhibitor of orphan estrogen-receptor-related (ERR) nuclear receptors beta and gamma. Endocrinology 142: 4572–4575.

Tremblay GB, Kunath T, Bergeron D, Lapointe L, Champigny C, Bader J-A *et al*. (2001b). Diethylstilbestrol regulates trophoblast stem cell differentiation as a ligand of orphan nuclear receptor ERRβ. Genes Dev 15: 833–838.

Tremblay AM, Wilson BJ, Yang XJ, Giguère V (2008). Phosphorylation-dependent sumoylation regulates estrogen-related receptor-α and -γ transcriptional activity through a synergy control motif. Mol Endocrinol 22: 570–584.

Vanacker JM, Delmarre C, Guo X, Laudet V (1998). Activation of the osteopontin promoter by the orphan nuclear receptor estrogen receptor related alpha. Cell Growth Differ 9: 1007–1014.

Vandewalle C, Van Roy F, Berx G (2009). The role of the ZEB family of transcription factors in development and disease. Cell Mol Life Sci 66: 773–787.

Van Gaal LF, Rissanen AM, Scheen AJ, Ziegler O, Rössner S, RIO-Europe Study Group (2005). Effects of the cannabinoid-1 receptor blocker rimonabant on weight reduction and cardiovascular risk factors in overweight patients: 1-year experience from the RIO-Europe study. Lancet 365: 1389–1397.

Vu EH, Kraus RJ, Mertz JE (2007). Phosphorylation-dependent sumoylation of estrogen-related receptor α1. Biochemistry 46: 9795–9804.

Wende AR, Huss JM, Schaeffer PJ, Giguère V, Kelly DP (2005). PGC-1alpha coactivates PDK4 gene expression via the orphan nuclear receptor ERRalpha: a mechanism for transcriptional control of muscle glucose metabolism. Mol Cell Biol 25: 10684–10694.

Wersto RP, Stetler-Stevenson M (1995). Debris compensation of DNA histograms and its effect on S-phase analysis. Cytometry 20: 43–52.

Willy PJ, Murray IR, Qian J, Busch BB, Stevens WC Jr, Martin R *et al.* (2004). Regulation of PPARgamma coactivator 1alpha (PGC-1α) signaling by an estrogen-related receptor α (ERRα) ligand. Proc Natl Acad Sci USA 101: 8912–8917.

Yang J, Williams RS, Kelly DP (2009). Bcl3 interacts cooperatively with peroxisome proliferator-activated receptor gamma (PPARγ) coactivator 1α to coactivate nuclear receptors estrogen-related receptor α and PPARα. Mol Cell Biol 29: 4091–4102.

Yin H, Chu A, Li W, Wang B, Shelton F, Otero F *et al.* (2009). Lipid G protein-coupled receptor ligand identification using beta-arrestin PathHunter assay. J Biol Chem 284: 12328–12333.

Zhu LL, Liu Y, Cui AF, Shao D, Liang JC, Liu XJ *et al.* (2010). PGC-1α coactivates estrogen-related receptor α to induce the expression of glucokinase. Am J Physiol Endocrinol Metab 298: E1210–E1218.

Supporting information

Additional Supporting Information may be found in the online version of this article:

Figure S1 (A) PANC-1 cells were serum starved for 3 h followed by treatment with vehicle (DMSO, 0.1%), AM251 (5 μM) or WIN 55212-2 (Win, 5 μM) for 24 h. Total RNA was isolated and analysed by quantitative PCR for the expression of EGFR and HB-EGF mRNAs. Values were normalized to 18S mRNA levels. The data represent three independent experiments. (B and C) PANC-1 cells were serum starved for 3 h followed by treatment with either vehicle, WIN 55212-2 (5 μM, B), AM251 (5 μM) or AM630 (5 μM) for 24 h. Total cell lysates were subjected to Western blot analysis using anti-EGFR antibody. GAPDH and β-tubulin were used as loading controls. The histograms in B and C represent the average ± range of two independent experiments.

Figure S2 Analysis of cell surface EGFR levels by flow cytometry. After treatment of PANC-1 cells with vehicle or AM251 (5 μM) for 24 h, aliquots of cells in suspension were incubated with anti-EGFR antibody followed by PE-labelled secondary antibody. A second group of cells were stained also with PE-conjugated mouse IgG as controls. Quantification of the mean peak values of cell surface EGFR ± AM251 was performed (right) for four independent experiments. Bars represent the average ± SEM with $^{**}P < 0.01$.

Figure S3 Effect of DES on EGFR and HB-EGF expression. (A) Serum-starved PANC-1 cells were incubated with DMSO or DES (1, 5, 20 μM) for 18 h. Real-time PCR was carried out for the determination of EGFR and HB-EGF mRNA levels. Values were normalized to 18S mRNA levels. Bars represent the average ± SD of two sets of dishes, each performed in duplicate. (B) Serum-starved PANC-1 cells were incubated with vehicle (DMSO) or DES (1, 5, 20 μM) for 18 h. Western blot analysis was carried out for the determination of EGFR and ERRα. The blots were reprobed for GAPDH expression as a loading control. Bars represent the average ± range of two dishes.

Table S1 List of the 10 highest expressed genes in AM251-treated PANC-1 cells

Please note: Wiley-Blackwell are not responsible for the content or functionality of any supporting materials supplied by the authors. Any queries (other than missing material) should be directed to the corresponding author for the article.